Expanded View Figures

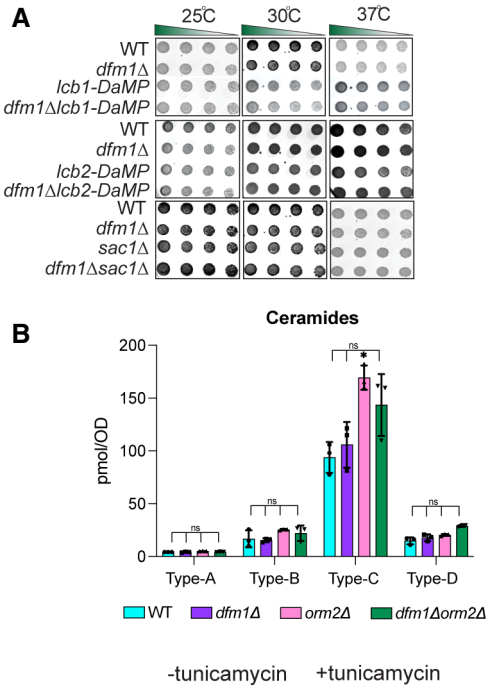

Figure EV1. Dfm1 does not genetically interact with Lcb1, Lcb2, and Sac1. Related to Fig 3.

A Indicated strains were spotted fivefold dilutions on SC plates in triplicates, and plates were incubated at room temperature, 30°C, and 37°C (3 biological replicates, 2 technical replicates; $n = 3$). *Upper panel*: WT, *dfm1*Δ, *Lcb1-DaMP*, *and dfm1*Δ*Lcb1*-DaMP were compared for growth by dilution assay. *Middle panel*: WT, *dfm1*Δ, *Lcb2-DaMP*, *and dfm1*Δ*Lcb2*-DaMP were compared for growth by dilution assay. *Bottom panel*: WT, *dfm1*Δ, *and dfm1*Δ *sac1*Δ were compared for growth by dilution assay.

B WT, *dfm1*Δ, *orm2*Δ, and *orm2*Δ*dfm1*Δ cells were grown to log phase at 30°C and lipids were extracted and subjected to LC–MS/MS. A-, B-, C-, and D-type ceramides containing C16, C18, C20, C22, C24, and C26 fatty acids were measured (3 biological replicates; $n = 3$). Values represent the means ± S.E.M. Statistically significant differences compared to WT cells are indicated (pairwise Dunnett's test followed by Bonferroni's *post hoc* analysis; ns, non-significant, $*P < 0.05$).

C Serial dilution growth was performed on YPD plates in the presence or absence of 1 μg/ml tunicamycin using WT, *orm1*Δ, *orm2*Δ, *dfm1*Δ, *dfm1*Δ*orm1*Δ, *orm1*Δ*orm2*Δ, and *dfm1*Δ*orm2*Δ cells (3 biological replicates, 2 technical replicates; $n = 3$).

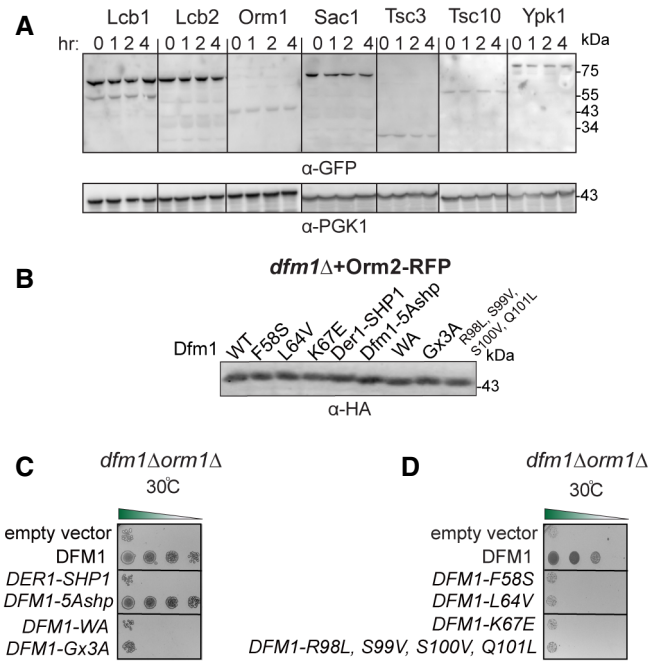

Figure EV2. Orm2 is degraded in WT strains. Related to Fig 5.

A In the indicated WT strains, degradation of Lcb1-GFP, Lcb2-GFP, Orm2-GFP, Orm2-GFP, Sac1-GFP, Tsc3-GFP, Tsc10-GFP, and Ypk1-GFP was measured by CHX-chase assay (3 biological replicates; $n = 3$). Cells were analyzed by SDS–PAGE and immunoblotted with α-GFP.

B Steady-state levels of Dfm1 and corresponding Dfm1 mutants. Cells were analyzed by SDS–PAGE and immunoblotted with α-HA.

C Serial dilution growth assay was performed on *dfm1Δorm1Δ* and strains with DFM1, DER1-SHP, DFM1-AA, DFM1-Ax3A, DFM1-5Ashpmtnt, and empty vector add back (3 biological replicates, 2 technical replicates; $n = 3$).

D Same as (C), except serial dilution growth assay was performed on *dfm1Δorm1Δ* strains with L1 mutant add back: F58S, L64V, K67E, and TMD2 quad mutant add back: DFM1-R98L, S99V, S100V, and Q101L. Indicated strains were grown on SC-Leu plates at room temperature, 30°C, and 37°C, and imaged on Day 2 and Day 7 (3 biological replicates, 2 technical replicates; $n = 3$).

E ERAD mutants do not genetically interact with *orm1Δ*. Indicated strains were spotted fivefold dilutions on SC plates in triplicate, and plates were incubated at room temperature, 30°C, and 37°C (3 biological replicates, 2 technical replicates; $n = 3$).

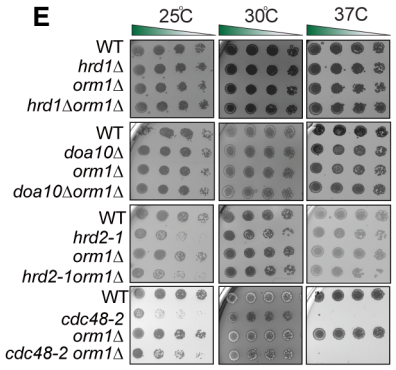

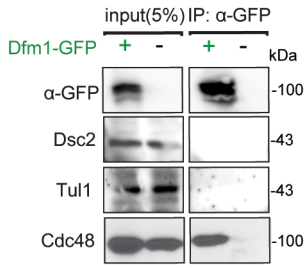

Figure EV3. Dfm1 does not interact with EGAD components. Related to Fig 6.

Dfm1-GFP binding to EGAD members, Dsc2 and Tul1, were analyzed by co-IP. As a negative control, cells not expressing Dfm1-GFP were used (2 biological replicates; $n = 2$).

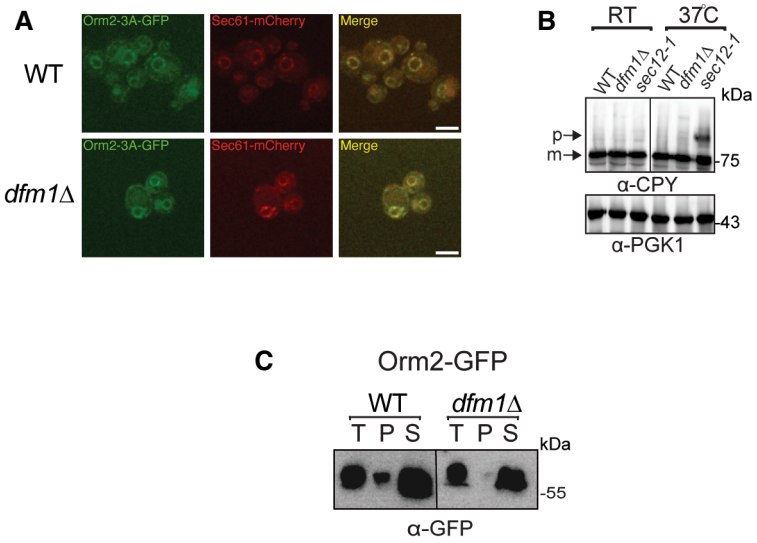

Figure EV4. Orm2-3A accumulates exclusively in the ER. Related to Fig 7.

A Fluorescence imaging was performed as in Fig 7B except for WT and *dfm1*Δ cells expressing Orm2-3A-GFP was used. Sec61-RFP (ER marker, red) was used to test for co-localization with Orm2-3A-GFP (2 biological replicates; $n = 2$). *Arrowheads* indicate Orm2 co-localizing in post-ER compartments. Scale bar, 5 μm.

B *dfm1*Δ cells do not abrogate COPII-mediated export of CPY. The indicated cells were either grown at room temperature or shifted to non-permissive growth at 37°C. Cells were analyzed by SDS–PAGE and immunoblotted for CPY with α-CPY and PGK1 with α-PGK1.

C Western blot of aggregated versus soluble Orm2-GFP at the ER. Lysates from WT and *dfm1*Δ cells containing ORM2-GFP were blotted using anti-GFP to detect Orm2. P is ER aggregated fraction and S is ER soluble fraction.